Electronic Supplementary Material (ESI) for Journal of Materials Chemistry A.


# Supplementary information

## Highly stretchable, self-adhesive, anti-freezing, and highly sensitive dual-network conductive hydrogel sensor for multifunctional electronic skin

Rui Zhang,[a] Di Xie,[a] Congcong Zhang,[a] Zesheng Xu,[a] Yiqun Fang,[a] Weihong Wang,[a] Min Xu,[a] Yongming Song[a,b]*

[a]Key Laboratory of Bio-based Material Science and Technology (Ministry of Education), College of Material Science and Engineering, Northeast Forestry University, Harbin 150040, P.R. China

[b]College of Home and Art Design, Northeast Forestry University, Harbin 150040, P.R. China

*Corresponding authors: ymsong@nefu.edu.cn

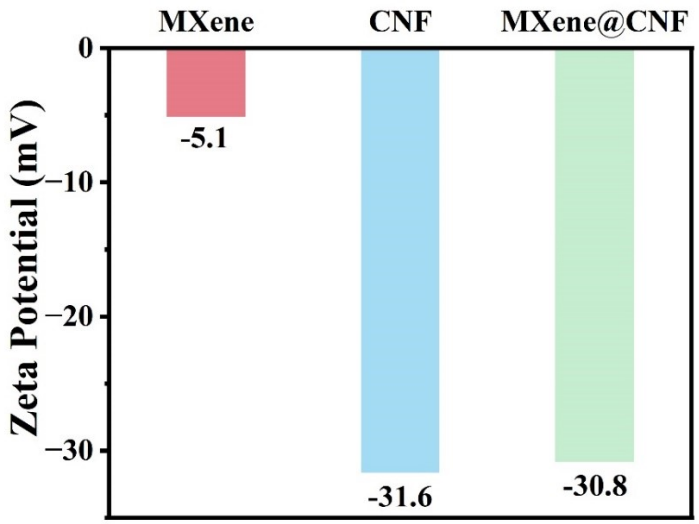


Figure S1. Zeta potential of aqueous solutions of MXene, CNF and MXene@CNF.

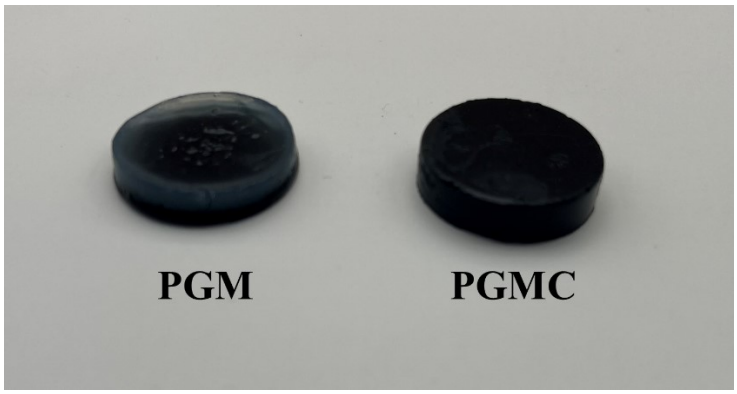


Figure S2. Photographs of PGM hydrogel and PGMC hydrogel.

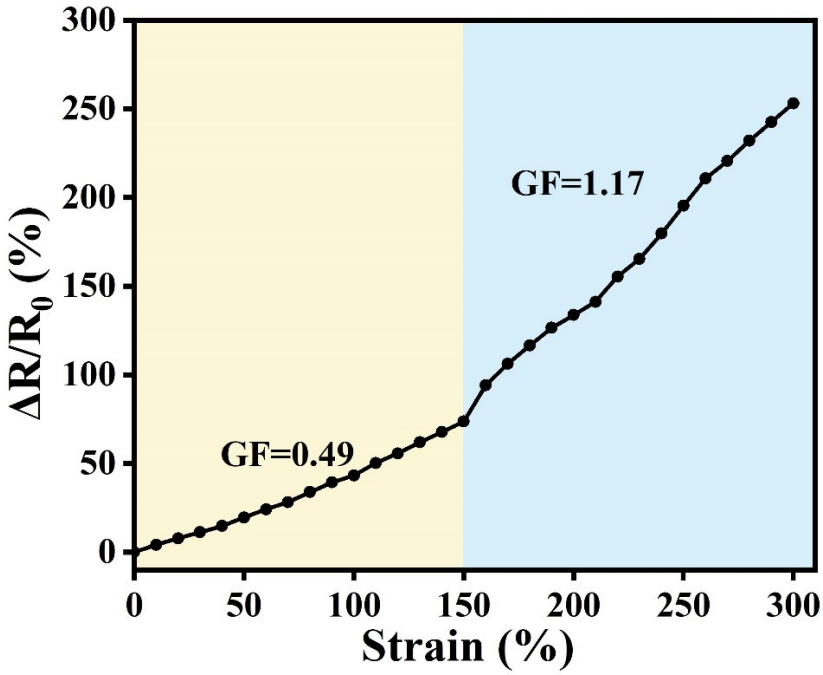


Figure S3. GF of the PGCa hydrogel sensor under different strains.

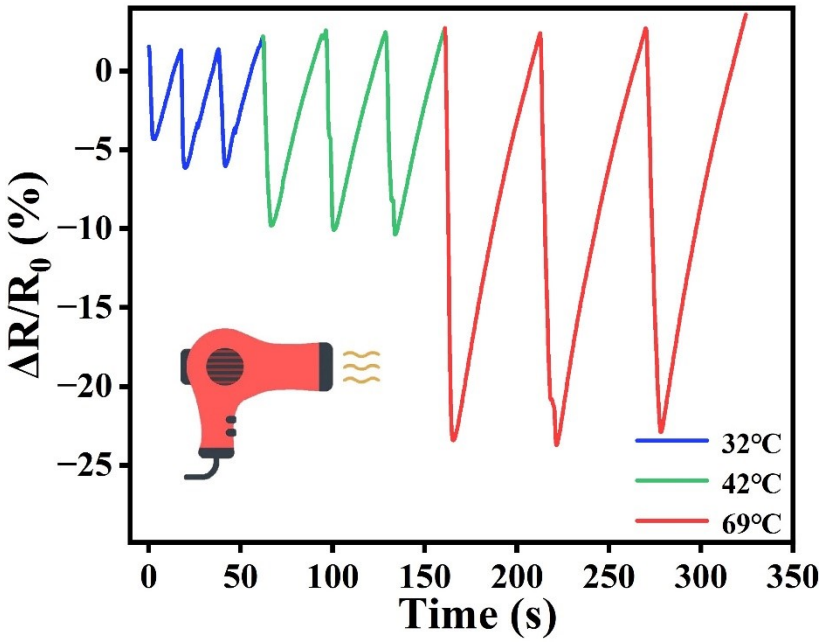


Figure S4. The PGMCCa hydrogel sensor monitors temperature changes in the hair dryer.

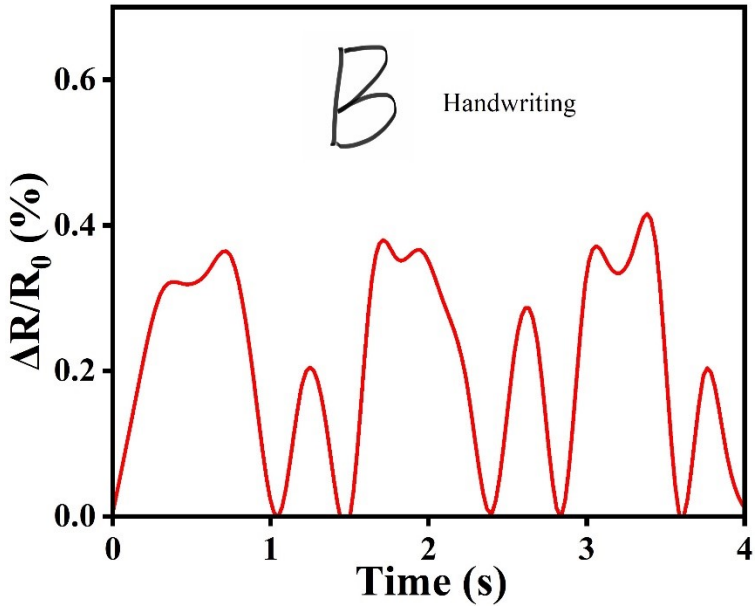


Figure S5. The resistance response of the sensor to write "B".

Table S1. Adhesion strength of different hydrogels.

| Material | Substrate | Adhesive strength (kPa) | References |
|---|---|---|---|
| Aa/CS/PAM/Fe(III) hydrogel | glass | 4.57 | [1] |
| PFeCNT-PAM hydrogel | glass | 15 | [2] |
| DA-QT-QP hydrogel | pigskin | 10 | [3] |
| MXene/Alg-DA/PAAm hydrogel | pigskin | 7.5 | [4] |
| PAA/Gelatin/TA/$Al^{3+}$ hydrogel | Al | 12.6 | [5] |
| CNC/PAA hydrogel | metal | 2.3 | [6] |
| **PGMCCa hydrogel** | **glass** | **20.2** | **This work** |
| **PGMCCa hydrogel** | **pigskin** | **17.4** | **This work** |
| **PGMCCa hydrogel** | **steel** | **23.1** | **This work** |

Table S2. X-band EMI shielding performance of typical shielding hydrogels.

| Samples | Filler content | EMI SE (dB) | Thickness (mm) | SE/d (dB/mm) | References |
|---|---|---|---|---|---|
| MXene/PVA hydrogel | 0.44 wt.% MXene | 25.6 | 2 | 12.8 | [7] |
| Cellulose/MXene hydrogel | MXene 5 mg/mL | 13.8 | 1 | 13.8 | [8] |
| PVA/EGaInSn–8Ni hydrogel | EGaInSn-Ni | 36 | 3 | 12 | [9] |
| PAM/CNF/MWCNT hydrogel | 0.1wt. %MWCNTs | 15 | 2 | 7.5 | [10] |
| **PGMCCa hydrogel** | **0.23 wt.%MXene** | **13.0** | **1** | **13.0** | **This work** |

Table S3. Gauge factor (GF), pressure sensitivity (S) and temperature coefficient of resistance (TCR) of hydrogel strain sensors.

| Samples | GF | S ($kPa^{-1}$) | TCR (%/°C) | References |
|---|---|---|---|---|
| CNTs/HAPAAm | 2.00(0-250%),<br>4.32(250-1000%) | 0.127 | | [11] |
| PNDU-CNF@CNT | 1.02(0–60%),<br>1.40(60–140%),<br>2.12(140–200%) | 1.11 | | [12] |
| PAAm/Gelatin/$Na_3Cit$ | 2.04(0–600%) | 0.0124 | | [13] |
| Starch/PAM | 0.98(0–50%) | 0.76 | | [14] |
| SA/GO/PAM | 4.2(0-2000%) | | 2.0 | [15] |
| PBGA | 0.989 | | 2.99 | [16] |
| STSMH | 37.59 | | 4.03 | [17] |
| PANI/gelatin | 1.4(0–764.4 %) | | 1.3 | [18] |
| AuNRs/PAA/PAM | 1.18(0–45%)<br>2.33(45–130%)<br>3.73(130–170%) | 6.75 | 1.252 | [19] |
| PVA-CNF | 0.96(0–100%)<br>1.57(100–300%) | 0.28 | 4.66 | [20] |
| **PGMCCa** | **4.56(0–100%),<br>10.44(100–200%),<br>40.43(200–500%)** | **1.026** | **3.30** | **This work** |

**Characterization**

1.X-ray photoelectron spectroscopy (XPS)

X-ray photoelectron spectroscope (XPS, Thermo Scientific, USA) was used to analyze the elemental and chemical composition of CNF and MXene@CNF. The XPS spectra were analyzed using an ESCALB 250Xi with a monochromatic Al Kα X-ray source, yielding a spot size of 380μm.

2.Zeta potential measurement

Zeta potential and size of CNF and different proportions of MXene@CNF (0.2 g/100 g aqueous) was measured using a Malvern Zeta sizer Nano series (ZEN 3600, Malvern Instruments, UK). The measurements were conducted three times.

3.Fourier transform infrared spectroscopy (FT-IR)

The molecular structure and chemical stability of the materials were tested and characterized by Fourier transform infrared (FT-IR) spectroscopy (NICOLET 6700). After freeze-drying, the FT-IR spectra were collected in the absorption mode at a resolution of 4 $cm^{-1}$. Each sample was scanned 64 times over a wavelength range of 4000–600 $cm^{-1}$. All tests were repeated three times.

4.Scanning electron microscopy (SEM)

The cross-sectional morphology of PGMCCa hydrogels was analyzed with a scanning electron microscope (JSM-7500F, Japan Electronics, Japan). Prior to characterization, hydrogel samples were first freeze-dried and brittle fractured in cryogenic liquid nitrogen. The hydrogel was fixed on the conductive glue and used to spray gold on the cross sections. The cross-sectional morphology of the samples was analyzed via SEM at an acceleration voltage of 5 kV.

5.Adhesion test

Bond strength was measured via the lap shear adhesion test. First, two identical pigskin plates with overlapping ends were glued with the PGMCCa hydrogel. The contact area between PGMCCa hydrogel and pigskin was 20 × 20 mm and the deformation rate was set at 30 mm/min. The adhesion strength(kPa) was calculated using Eq. (1):

$$\text{Adhesion strength(kPa)} = (\text{maximum load (N)}) / (\text{the contact area}(mm^2)) \quad (1)$$

The adhesion strength of the hydrogels to pigskin, steel, rubber and glass was evaluated in a similar method, and each sample was tested three times.

6.Rheology testing

The dynamic rheological properties of the materials were evaluated with a rotating rheometer (AR2000ex, TA instruments, New Castle, De, USA). Parallel plates of 25 mm diameter were selected for testing under the following parameters: a gap of 1000μm, a temperature of 25°C, a strain of 1% (in the linear viscoelastic region), and a frequency range of 600–0.1 rad/s. Each sample was analyzed in triplicate. The curves of the storage modulus (G') and the loss modulus (G'') with the angular frequency of the hydrogel samples were obtained.

7.Mechanical test

Mechanical tests were performed using a digital tensile tester (CMT5504, MTS system, China) equipped with a 2 kN loading cell. The hydrogel was made into a dumbbell-shaped sample with a gauge length of 75 mm, width of 5 mm, and a thickness of 1 mm. The tensile tests were conducted at a loading rate of 60mm/min. The compression test was performed on a cylindrical sample measuring 20 mm in diameter and 15 mm in height at a speed of 5 mm/min. All samples were tested three times and the average was taken. Toughness and Young's modulus were obtained by calculating the integral area and initial slope (between elongation ~5% and ~20%) of the stress-strain curve, respectively.

8.Anti-freezing and moisture retention property tests

The anti-freezing properties of the samples were analyzed by differential scanning calorimetry (DSC TA Q20). Hydrogel samples were cooled from 30°C to −80°C at 10°C/min under a nitrogen flow rate of 50mL/min, maintained for 5min, then heated to 30°C at the same rate. The freezing point of the hydrogel was defined as the peak value during the heating process. The moisture retention properties of the samples were tested for weight change at room temperature with 40% RH for 7 days.

9.Conductivity test

We measured the conductivity of the hydrogels using an LCR digital bridge

(TH2830, Changzhou, China). The conductivity (σ, S/m) was calculated using Eq. (2):

$$\sigma=L/(R\times S) \quad (2)$$

In Eq. (2) above, *L* is the distance between the electrodes; *R* denotes the resistance of the sample; and *S* represents the cross-sectional contact area of the sample.

The real-time change in the resistance of different strains was measured using the LCR digital bridge. The voltage was 1V, and the scanning frequency was 1kHz. In the mechanical tensile testing, the resistance of the hydrogel was measured using a digital tensile tester (CMT5504, MTS system, China) based on the change in tensile strain. The temperature were 25°C and -20°C, and the hydrogel sample dimensions were 75mm×5mm×1mm. The hydrogel samples (-20°C) were frozen at -20°C for 24 hours prior to testing.

The relative resistance change rate (%) was calculated using Eq. (3):

$$\text{Relative resistance change rate}=(R-R_0)/R_0\times 100\%=\Delta R/R_0\times 100\% \quad (3)$$

where $R_0$ is the initial resistance of the hydrogel sample. $R$-$R_0$ is the change in the resistance during hydrogel stretching.

The strain sensitivity of hydrogels was evaluated based on the gauge factor (GF) using Eq. (4):

$$GF=(\Delta R/R_0)\div\varepsilon \quad (4)$$

where ε is the strain.

10.EMI Shielding Test of PGMCCa Hydrogel

According to the Institute of Electrical and Electronic Engineers Standard 521, the X-band is defined as the radio wave band with a frequency of 8-12 GHz[21]. The EMI SE of the PGMCCa hydrogel (30×30 $mm^2$) was measured by the vector network analyzer (Keysight E5071C) in 8.2–12.4 GHz (X band). It was calculated from the scattering parameters ($S_{11}$ and $S_{21}$) by the following equation [8]:

$$SE_T = SE_R + SE_A + SE_M \quad (5)$$

$$SE_R = -10log\left(1-|S_{11}|^2\right) \quad (6)$$

$$SE_A = -10log\left(\frac{|S_{21}|^2}{1-|S_{11}|^2}\right) \quad (7)$$

where $SE_T$ is the total SE, $SE_R$ is the reflection SE and $SE_A$ absorption SE. SEM is the multiple reflections shielding, which will negligible when $SE_T \geq 15dB$[10].

## References


1. J. Ren, M. Li, X. M. Wang, Y. Li and W. Yang, *Polym. Bull.*, 2023, **80**, 1335-1351.
2. K. Liu, L. Han, P. Tang, K. Yang, D. Gan, X. Wang, K. Wang, F. Ren, L. Fang, Y. Xu, Z. Lu and X. Lu, *Nano Lett.*, 2019, **19**, 8343-8356.
3. L. Wang, Z. Zhao, J. Dong, D. Li, W. Dong, H. Li, Y. Zhou, Q. Liu and B. Deng, *ACS Appl. Mater. Interfaces*, 2023, **15**, 16515-16525.
4. X. X. Wu, H. Liao, D. Ma, M. Y. Chao, Y. G. Wang, X. L. Jia, P. B. Wan and L. Q. Zhang, *J. Mater. Chem. C*, 2020, **8**, 1788-1795.
5. Z. He and W. Yuan, *ACS Appl. Mater. Interfaces*, 2021, **13**, 1474-1485.
6. W. Ma, W. Cao, T. Lu, Z. Jiang, R. Xiong, S. K. Samal and C. Huang, *ACS Appl. Mater. Interfaces*, 2021, **13**, 58048-58058.
7. Y. F. Yang, B. Li, N. Wu, W. Liu, S. Y. Zhao, C. J. Zhang, J. R. Liu and Z. H. Zeng, *ACS Materials Lett.*, 2022, **4**, 2352-2361.
8. Y. Bai, S. Bi, W. Wang, N. Ding, Y. Lu, M. Jiang, C. Ding, W. Zhao, N. Liu, J. Bian, S. Liu and Q. Zhao, *Soft Mater.*, 2022, **20**, 444-454.
9. B. Zhao, Z. Bai, H. Lv, Z. Yan, Y. Du, X. Guo, J. Zhang, L. Wu, J. Deng, D. W. Zhang and R. Che, *Nano-micro Lett,*, 2023, **15**, 79.
10. W. Yang, B. Shao, T. Liu, Y. Zhang, R. Huang, F. Chen and Q. Fu, *ACS Appl Mater Interfaces*, 2018, **10**, 8245-8257.
11. Z. Qin, X. Sun, Q. Yu, H. Zhang, X. Wu, M. Yao, W. Liu, F. Yao and J. Li, *ACS Appl. Mater. Interfaces*, 2020, **12**, 4944-4953.
12. L. Jia, S. Wu, R. Yuan, T. Xiang and S. Zhou, *ACS Appl. Mater. Interfaces*, 2022, **14**, 27371-27382.
13. X. Sun, F. Yao, C. Wang, Z. Qin, H. Zhang, Q. Yu, H. Zhang, X. Dong, Y. Wei and J. Li, *Macromol. Rapid Commun.*, 2020, **41**, e2000185.
14. S. Zeng, J. Y. Zhang, G. Q. Zu and J. Huang, *Carbohydr. Polym.*, 2021, **267**, 118198.
15. W. W. Hou, Z. H. Luan, D. Xie, X. H. Zhang, T. B. Yu and K. Y. Sui, *Compos. Commun.*, 2021, **27**, 100837.
16. X. R. Yu, W. J. Qin, X. X. Li, Y. L. Wang, C. S. Gu, J. J. Chen and S. G. Yin, *J. Mater. Chem. A*, 2022, **10**, 15000-15011.
17. L. Bai, Y. Jin, X. Shang, H. Y. Jin, L. J. Shi, Y. P. Li and Y. T. Zhou, *Nano Energy*, 2022, **104**, 107962.
18. S. Sun, F. Y. Hao and X. Maimaitiyiming, *ChemistrySelect*, 2022, **7**, 8.
19. X. Y. Qu, J. Y. Liu, S. Y. Wang, J. J. Shao, Q. Wang, W. J. Wang, L. Gan, L. P. Zhong, X. C. Dong and Y. X. Zhao, *Chem. Eng. J.*, 2023, **453**, 139785.
20. M. Li, D. Chen, X. Sun, Z. Xu, Y. Yang, Y. Song and F. Jiang, *Carbohydr. Polym.*, 2022, **284**, 119199.

21. F. Ruiz-Perez, S. M. Lopez-Estrada, R. V. Tolentino-Hernandez and F. Caballero-Briones, *J Sci-Adv Mater Dev*, 2022, **7**, 100454.